

ble of Isotopes (Wiley, New York, 1967), 6th ed.

<sup>4</sup>R. Brandt, in *Proceedings of the Symposium on the Physics and Chemistry of Fission, Salzburg, 1965* (International Atomic Energy Agency, Vienna, Austria, 1965), Vol. 2, p. 329.

<sup>5</sup>K. Beg and N. T. Porile, *Phys. Rev. C* **3**, 1631 (1971).

<sup>6</sup>E. Hagebø and H. Ravn, *J. Inorg. Nucl. Chem.* **31**, 2649 (1969).

<sup>7</sup>J. B. Cumming, *Ann. Rev. Nucl. Sci.* **13**, 261 (1963).

<sup>8</sup>Y. Y. Chu, E. M. Franz, and G. Friedlander, to be published.

<sup>9</sup>J. H. Davies and L. Yaffe, *Can. J. Phys.* **41**, 762 (1963).

<sup>10</sup>K. M. Broom, *Phys. Rev.* **133**, B874 (1964).

<sup>11</sup>Y. Y. Chu, University of California Radiation Laboratory Report No. UCRL-8926, 1959 (unpublished).

PHYSICAL REVIEW C

VOLUME 4, NUMBER 5

NOVEMBER 1971

## Photoneutron Cross Sections for <sup>23</sup>Na and <sup>25</sup>Mg†

R. A. Alvarez, B. L. Berman, D. R. Lasher, T. W. Phillips, and S. C. Fultz  
Lawrence Radiation Laboratory, University of California, Livermore, California 94550

(Received 15 June 1971)

Nearly monochromatic photons from positron annihilation in flight have been used to measure photoneutron cross sections for <sup>23</sup>Na and <sup>25</sup>Mg in the giant-resonance region. The shape of the giant resonance of each of these nuclei is rather broad, with less striking intermediate structure than in most neighboring *sd*-shell nuclei. In <sup>23</sup>Na the total cross section rises to approximately 10 mb at 17.5 MeV and remains essentially constant up to 25 MeV. In <sup>25</sup>Mg the total cross section reaches a peak of 28 mb at 23.1 MeV and falls to approximately half that magnitude at the upper energy limit of the experiment (29 MeV). In both nuclei the ( $\gamma, 2n$ ) cross section appears to rise slowly above threshold but does not exceed 1 mb within the energy limits of the experiment. The integrated cross sections for <sup>23</sup>Na and <sup>25</sup>Mg are 119 and 249 MeV mb, respectively; the bremsstrahlung-weighted integrated cross sections are 5.7 mb for <sup>23</sup>Na and 11.7 mb for <sup>25</sup>Mg.

### I. INTRODUCTION

Nearly monochromatic photons from in-flight annihilation of positrons from the Livermore electron linac have been used to investigate photoneutron cross sections for a number of deformed light nuclei. Results have been published previously<sup>1,2</sup> for <sup>27</sup>Al and <sup>28</sup>Si; new results for <sup>24</sup>Mg and <sup>26</sup>Mg appear in a separate paper.<sup>3</sup>

In the present paper we report the results of measurements of photoneutron cross sections for <sup>23</sup>Na and <sup>25</sup>Mg.

### II. EXPERIMENTAL PROCEDURE

The experimental technique used for the measurements described herein was similar to that employed in the <sup>27</sup>Al experiment,<sup>1</sup> and the neutron detector and electronics were essentially identical. The beam transport system, however, was modified. The new transport system, shown in Fig. 1, consisted of two 90° bending magnets and several quadrupole lenses which carried the positron beam from the accelerator through a total bend of 180° and focused it onto a 0.010-in.-thick beryllium annihilation target. On nearly all runs more than 95% of the positron beam fell within the 0.50-in.

diameter of the annihilation target. The residual positron beam transmitted through the annihilation target was carried through a 49° bend by a sweeping magnet into a carbon beam dump.

The main contributions to the width of the photon energy resolution come from energy losses by the positrons in the beryllium before annihilation, the angular collimation of the photon beam together with multiple scattering, the energy-angle relationship in the annihilation kinematics, and the energy spread of the incident positron beam. The last of these was chosen to be 1% for the present experiment (and for the <sup>26</sup>Mg experiment<sup>3</sup>) by energy-defining slits located between the two bending magnets in the transport system. The effects of energy loss and scattering in the annihilation target have been discussed in previous publications,<sup>4</sup> and the expected photon energy resolution for a 0.010-in.-thick beryllium target is tabulated by Bramblett *et al.*<sup>5</sup> The resolution varies between 1.05 and 1.30% over the giant-resonance energy region. The resolution was checked in the experimental configuration used for the present experiment by measuring the width of the 17.28-MeV photoneutron peak in <sup>16</sup>O. Furthermore, a separate experiment<sup>3</sup> with the identical experimental setup has shown that the observed widths of two low-energy peaks in <sup>26</sup>Mg are consistent with the

resolutions given in Ref. 5; the natural widths of these peaks are known precisely from threshold photoneutron measurements.<sup>6</sup> The energy calibration of the beam transport system was determined primarily by measuring the magnetic field in the bending magnets at the 17.28-MeV resonance, the absolute energy of which is known accurately from neutron time-of-flight measurements.<sup>7</sup>

The photon beam emerging from the annihilation target passed through a set of lead collimators and a spherical ion-chamber beam monitor, and irradiated the sample located at the center of the neutron detector. The integrated charge per annihilation photon from the ion-chamber monitor was calibrated previously against the number of counts in the annihilation peak in an 8-in.-thick by 8-in.-diameter NaI(Tl)  $\gamma$ -ray spectrometer as a function of annihilation-photon energy. The integrated charged-particle beam current incident on the annihilation target also was monitored during each run by collecting the secondary electrons emitted from the beryllium. The small effect of attenuation of the incident photon beam as it passed through the neutron sample (owing to absorption by the material in the sample) was taken into account in the data-reduction program.

The neutron detector used in this experiment consists of a 2-ft cube of paraffin moderator in which are imbedded 48 20-in.-long  $\text{BF}_3$  detectors. The latter are arranged in an array of four coaxial rings, each containing 12 tubes, cylindrically symmetric about the beam line (which passes through

a 3-in.-diameter cylindrical hole through the center of the paraffin cube). For a given annihilation-photon energy the ratio of counts in the inner and outer rings gives the average neutron energy and also the detector efficiency. The detector efficiency and counting-rate ratios of the rings of  $\text{BF}_3$  tubes were measured previously as a function of average neutron energy with calibrated sources. The efficiency was checked at least once a day during data runs with one of the sources. Further details of the detector are given in previous publications from this laboratory.<sup>8</sup>

In addition to recording the number of neutron counts in each detector ring, the electronics associated with the experiment recorded the number of events in which one, two, three, etc., neutrons were detected within a 300- $\mu$ sec gate which opened a few microseconds after each beam pulse. A statistical analysis of the multiplicity counts gave information on the  $(\gamma, 2n)$ ,  $(\gamma, 3n)$ , etc., cross sections as well as the  $(\gamma, n)$  cross section. The delay between the beam pulse and the start of the gate was necessary to avoid spurious counts caused by  $\gamma$  flash in the detectors and rf pickup from the accelerator by the preamplifiers. In the present measurement the delay was set at 8  $\mu$ sec, and the small effect on the detector efficiency has been taken into account.

The  $^{25}\text{Mg}$  sample consisted of 49.77 g of  $\text{MgO}$  with the isotopic content enriched to 97.87%. The major impurity was approximately 2%  $^{24}\text{Mg}$ . The  $^{23}\text{Na}$  sample consisted of 154 g of sodium metal.

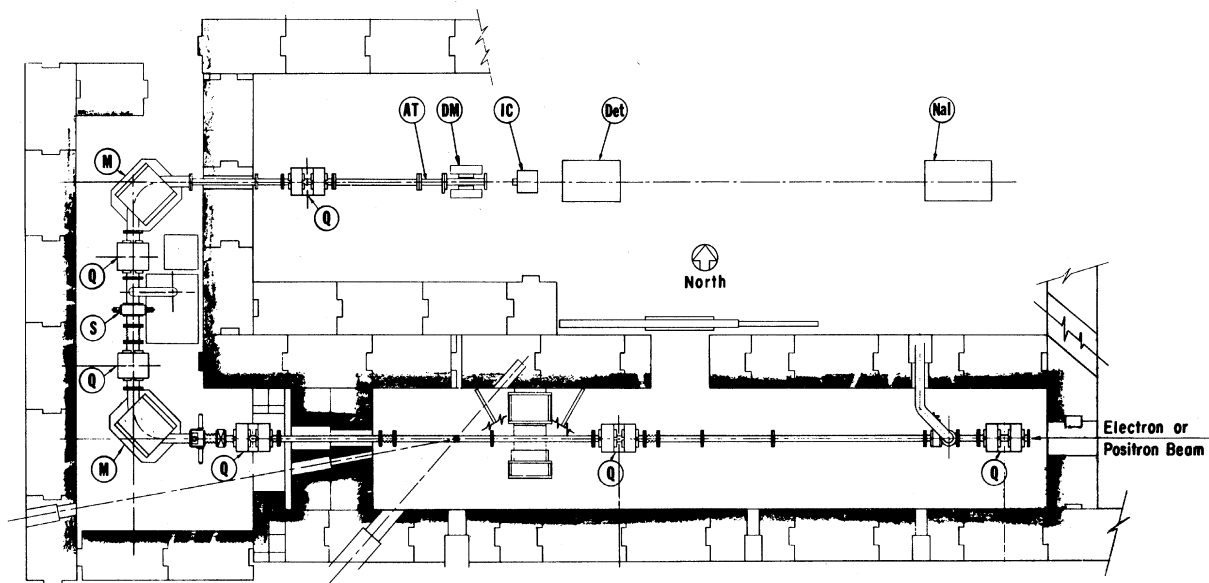


FIG. 1. Plan view of the beam transport system and experimental apparatus, showing the location of quadrupoles Q, bending magnets M, energy-defining slits S, annihilation target AT, beam-dump magnet DM, ion chamber IC, and neutron detector Det; the sodium iodide detector NaI was used for beam calibration.

Both samples were encapsulated in 1.75-in.-diam-eter thin-walled Lucite cylinders which were held centered in the neutron detector in Styrofoam holders. For background measurements, duplicate capsules and holders were used. In the case of  $^{25}\text{MgO}$ , an amount of water containing the same mass of oxygen was included in the "blank" capsule so that the photoneutron contribution from oxygen would be subtracted out automatically, along with other backgrounds.

The complete set of data for each isotope consisted of four sets of runs. These included runs for both the sample and blank sample holder, with both positrons and electrons incident on the annihilation target in each case. The runs with inci-

dent electrons, appropriately normalized, provided data for subtracting the neutron yields caused by the bremsstrahlung flux which accompanied the nearly monochromatic annihilation radiation during the positron runs. Since the neutron yield from bremsstrahlung is a relatively smooth, monotonic function of beam energy, an adequate subtraction of the bremsstrahlung-induced yield was possible with relatively widely spaced incident-electron data. Subtraction of the neutron yield from the oxygen in the  $^{25}\text{MgO}$  sample was achieved with the data from the water-loaded "blank" sample holder, augmented by knowledge of the shape of the oxygen giant resonance from previously published data.<sup>2,9</sup>

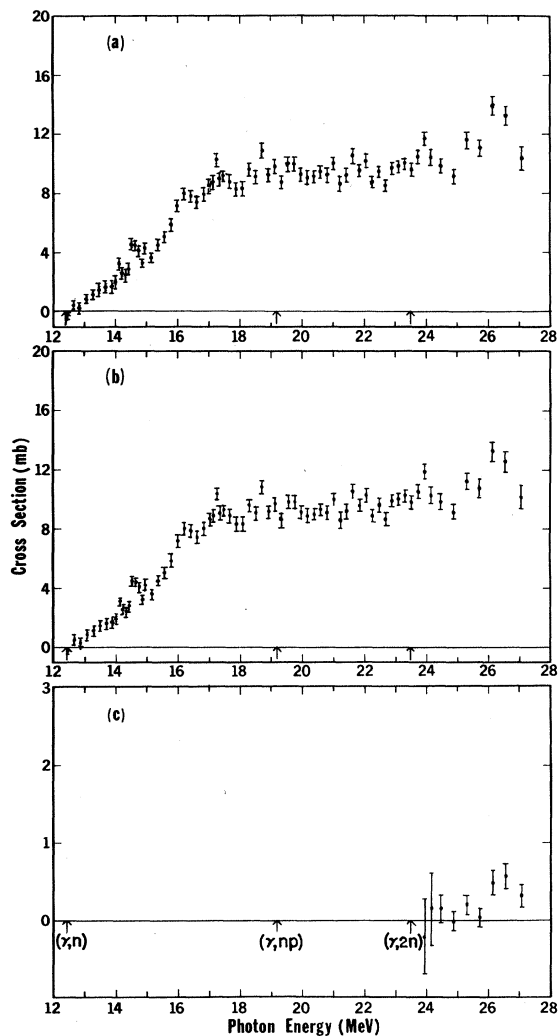


FIG. 2. Cross sections for  $^{23}\text{Na}$ . (a) Total photoneutron cross section,  $\sigma[(\gamma,n) + (\gamma,np) + (\gamma,2n)]$ . (b) Single-photoneutron cross section,  $\sigma[(\gamma,n) + (\gamma,np)]$ . (c) Double-photoneutron cross section,  $\sigma(\gamma,2n)$ . The thresholds (arrows) are taken from Mattauch *et al.* (see Table I).

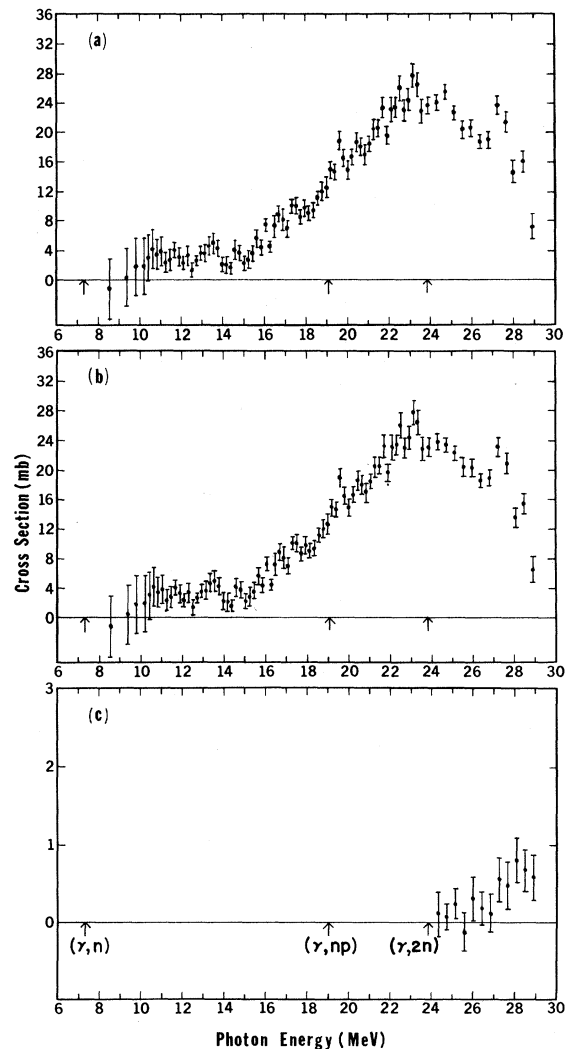


FIG. 3. Cross sections for  $^{25}\text{Mg}$ . (a) Total photoneutron cross section,  $\sigma[(\gamma,n) + (\gamma,np) + (\gamma,2n)]$ . (b) Single-photoneutron cross section,  $\sigma[(\gamma,n) + (\gamma,np)]$ . (c) Double-photoneutron cross section,  $\sigma(\gamma,2n)$ .

### III. EXPERIMENTAL RESULTS

The measured cross sections are shown for  $^{23}\text{Na}$  in Fig. 2 and for  $^{25}\text{Mg}$  in Fig. 3. Since the experimental technique employed was insensitive to the emission of protons, the "single-photon-neutron" cross sections include  $\sigma(\gamma, np)$  as well as  $\sigma(\gamma, n)$ ; an analogous statement holds for the "double-photon-neutron" cross section. All particle emission thresholds below 30 MeV are listed in Table I, and the  $(\gamma, n)$ ,  $(\gamma, np)$ , and  $(\gamma, 2n)$  thresholds are indicated in the figures by arrows.

The general shape of the cross section for  $^{23}\text{Na}$  is a steady rise from threshold to an essentially flat plateau extending from 17.5 to 25 MeV with a magnitude of about 10 mb. The  $(\gamma, 2n)$  cross section appears to remain close to zero for approximately 2 MeV above threshold, followed by a possible peaking at 26.5 MeV, where a peaking in the  $(\gamma, n)$  cross section also seems to occur; it remains generally small, however, up to the energy limits of the experiment.

For  $^{25}\text{Mg}$  the cross section rises slowly from threshold to approximately 3 mb at 10 MeV and fluctuates slightly about that value up to 15 MeV, where it begins rising toward a peak of 28 mb at 23.1 MeV. Above the peak energy the cross section begins a decline to roughly half the peak value at the energy limit of the experiment (29 MeV). The  $(\gamma, 2n)$  cross section for  $^{25}\text{Mg}$  begins to rise significantly about 3 MeV above threshold, but remains smaller than 1 mb up to 29 MeV.

An attempt at fitting the present data with a series of resonance curves did not seem warranted because of the absence of strong structure. It is possible, however, to identify several small but well-defined peaks on the rising edges of the giant resonance. These occur, in  $^{23}\text{Na}$ , at approximately 14.1, 14.6, 16.3, 17.3, and 18.8 MeV, and in  $^{25}\text{Mg}$  at 13.5 and 19.6 MeV. In addition, there are smaller fluctuations which are less readily identified, especially in  $^{25}\text{Mg}$  in the 14–18-MeV region and near 11.7 MeV. The latter might be associated with the peak seen in  $180^\circ$  electron scattering<sup>10</sup> at

TABLE I. Photonuclear reaction thresholds for  $^{23}\text{Na}$  and  $^{25}\text{Mg}$ , J. H. E. Mattauch, W. Thiele, and A. H. Wapstra, Nucl. Phys. **67**, 32 (1965).

Reaction	$^{23}\text{Na}$	$^{25}\text{Mg}$
$(\gamma, n)$	12.418	7.329
$(\gamma, p)$	8.792	12.061
$(\gamma, np)$	19.159	19.023
$(\gamma, 2p)$	24.061	22.62
$(\gamma, 2n)$	23.487	23.861
$(\gamma, n2p)$	32.166	27.815
$(\gamma, p2n)$	25.919	31.4

an excitation energy of 11.76 MeV and attributed to an M1 transition.

Previous determinations of the gross shape of the giant resonance have been made via photoneutron production with bremsstrahlung beams by Sato<sup>11</sup> and Fielder, Bolen, and Whitehead<sup>12</sup> for  $^{23}\text{Na}$ , and by Nathans and Yergin<sup>13</sup> for  $^{25}\text{Mg}$ . Although their resolution is considerably coarser, the main features indicated by the previous experiments are not inconsistent with the present result, except for a premature falling-off of the data of Sato<sup>11</sup> and Nathans and Yergin<sup>13</sup> at the higher energies (see Fig. 4). The data of Fielder, Bolen, and Whitehead<sup>12</sup>, which extend above 30 MeV, are consistent with the present measurement throughout the common energy range except for perhaps a 10% discrepancy in over-all normalization.

The integrated cross sections, obtained with a linear interpolation between data points, are shown in Table II. The values of  $\sigma_{\text{int}}$  for  $^{23}\text{Na}$  and  $^{25}\text{Mg}$  are 35 and 67% of the predictions of the dipole sum rule (60NZ/A MeV mb), respectively. For nuclei in this mass region, the  $(\gamma, p)$  reaction probably contributes significantly to the sum rule. Photoproton data for  $^{25}\text{Mg}$  by Katz *et al.*,<sup>14</sup> for example, give an integrated cross section of 120 MeV mb, which, when added to the present photoneutron results, essentially exhausts the sum rule. The photoneutron cross section for  $^{23}\text{Na}$ , furthermore, contributes significantly to the sum rule up to considerably higher energies, as is shown by the results of Fielder, Bolen, and Whitehead.<sup>12</sup>

### IV. DISCUSSION

The major qualitative features of the giant resonance for  $^{23}\text{Na}$  and  $^{25}\text{Mg}$  are the rather broad peaks with little striking intermediate structure, and the small magnitude of the  $(\gamma, 2n)$  cross section for approximately the first 5 MeV above threshold. Both of these features also are observed in the data on  $^{27}\text{Al}$ , the other odd-*A* nucleus in this series of measurements.<sup>1</sup> In all three cases, there are some discernible peaks superimposed on the broad structure of the giant resonance, particularly on the rising edge. The intermediate structure, however, is not nearly so striking as that observed<sup>2,3</sup> in the even-*A* isotopes of the series,  $^{24}\text{Mg}$ ,  $^{26}\text{Mg}$ , and  $^{28}\text{Si}$ , in which the magnitude of the fluctuations in the cross section are of the same order as the average value. These results raise the question of whether it is a general feature of nuclei in this mass region that the giant resonance for even-*A* nuclei exhibits a generally richer structure than for those with odd mass number. Unfortunately there has not been enough experimental investigation of the odd-*A* nuclei in this region with ade-

quate resolution either by photodisintegration experiments or by the inverse capture reactions to answer the question definitively.

The presence of prominent intermediate structure in the giant-resonance region in a number of even- $A$   $sd$ -shell nuclei is either indicated or confirmed by several other experiments. Total absorption cross sections have been measured<sup>15</sup> for  $^{24}\text{Mg}$  and  $^{40}\text{Ca}$ .  $^{28}\text{Si}$  has been investigated via the  $(p, \gamma)$  process<sup>16</sup> and photoneutron experiments.<sup>17</sup> Proton-capture experiments have also been used to study  $^{20}\text{Ne}$ <sup>18</sup> and  $^{24}\text{Mg}$ .<sup>19</sup> In the latter, as well as in  $^{26}\text{Mg}$ , marked structure in the giant reso-

nance also has been observed in inelastic electron-scattering experiments,<sup>20</sup> especially at the more forward angles where  $E1$  transitions overwhelm those of magnetic origin.  $^{40}\text{Ca}$  and  $^{32}\text{S}$  have been investigated with photonuclear experiments<sup>17, 21-24</sup> and the latter also has been studied by radiative proton capture<sup>25</sup> on  $^{31}\text{P}$ . A number of  $sd$ -shell nuclei ( $^{19}\text{F}$ ,  $^{20}\text{Ne}$ ,  $^{27}\text{Al}$ ,  $^{36}\text{Ar}$ ,  $^{40}\text{Ar}$ , and  $^{39}\text{K}$ ) have been investigated<sup>26</sup> in bremsstrahlung-induced  $(\gamma, p)$  reactions in which the proton-energy spectra were measured. In these experiments the excitation function is deduced under the assumption that ground-state transitions are dominant; the shape

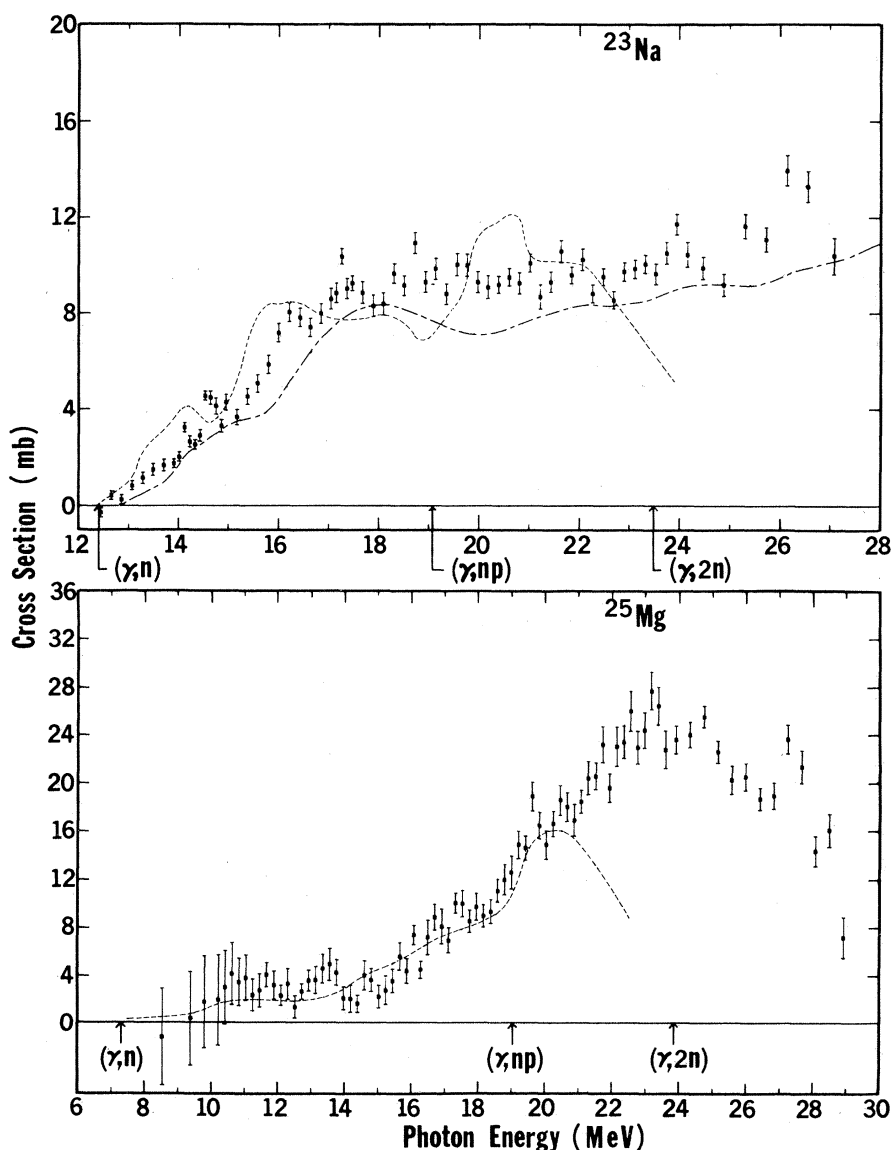


FIG. 4. Comparison of the present total photoneutron cross sections with previous measurements. The dashed curves indicate the results of Sato (Ref. 11) for  $^{23}\text{Na}$  and of Nathans and Yergin (Ref. 13) for  $^{25}\text{Mg}$ ; the dash-dot curve represents the  $^{23}\text{Na}$  data of Fielder, Bolen, and Whitehead (Ref. 12).

TABLE II. Integrated total photoneutron cross sections and their moments.

Nucleus	$E_{\gamma\max}$ (MeV)	$\sigma_{\text{int}}^a$ (MeV mb)	$\sigma_{-1}^b$ (mb)	$\sigma_{-2}^b$ (mb MeV <sup>-1</sup> )
<sup>23</sup> Na	27	119	5.74	0.288
<sup>25</sup> Mg	29	249	11.7	0.584

<sup>a</sup>  $\sigma_{\text{int}} \equiv \int_{E_{\text{thr}}}^{E_{\gamma\max}} \sigma_{\text{tot}} dE.$   
<sup>b</sup>  $\sigma_{-n} \equiv \int_{E_{\text{thr}}}^{E_{\gamma\max}} \sigma_{\text{tot}} E^{-n} dE.$

thus obtained for the giant resonance is therefore not as unambiguous as is the case with  $(p, \gamma_0)$  measurements or photoneutron experiments with monoenergetic  $\gamma$  rays. The shapes of the proton spectra are not inconsistent, however, with the general qualitative observation, based primarily on the photoneutron measurements, that the odd- $A$  nuclei of the  $sd$  shell exhibit significantly less intermediate structure in the giant resonance than do those with even mass number.

Of course it is not surprising that the noted qualitative difference in the giant-resonance structure of the even- $A$  and odd- $A$  isotopes should exist. One would expect the presence of an unpaired nucleon to provide a richer spectrum of doorway states in the odd- $A$  nuclei, which could in fact wash out most of the structure when observed with a resolution of a few tens of keV or more.

The second major feature noted above, the small  $(\gamma, 2n)/(\gamma, n)$  cross-section ratio, also is not surprising since there are  $T=1$  levels well below the neutron separation energy in the daughter nuclei<sup>27</sup> (for example, at 0.66 and 1.95 MeV in <sup>22</sup>Na, and at 9.5 MeV in <sup>24</sup>Mg) to which either a  $T=\frac{1}{2}$  or  $T=\frac{3}{2}$  giant-resonance state can decay; these levels subsequently decay by  $\gamma$ -ray emission. The same is true of <sup>27</sup>Al, which also has a small  $(\gamma, 2n)$  cross section below 30 MeV. The relatively large  $(\gamma, 2n)$  cross section for <sup>26</sup>Mg can be explained in terms of isopin selection rules and isopin mixing in the  $T=\frac{3}{2}$  states of <sup>25</sup>Mg (see Ref. 3). Data on the  $(\gamma, 2n)$  reaction in other nuclei in this mass range are lacking.

It has long been postulated<sup>28</sup> that the giant resonance of a nucleus with  $N \neq Z$  should be split into two isospin components with an energy separation, in light nuclei, of a few MeV.<sup>29</sup> Conclusive evidence for isospin splitting of the giant resonance in <sup>26</sup>Mg into  $T=1$  and  $T=2$  components, with a separation of approximately 5 MeV, is contained in the data of Wu, Firk, and Berman,<sup>30</sup> combined with the aid of the data of Ref. 3; the argument is given in detail in Ref. 3.

Fallieros, Goulard, and Venter<sup>29</sup> have estimated

the energy splitting in several nuclei and found it to be characterized by the effective symmetry energy  $\bar{\nu} = 2T_0M$ , where  $T_0$  is the ground-state isospin and  $M$  is an effective transition matrix element which is to be taken as a constant for a given isotope. The characteristic isospin energy splitting then can be represented as

$$\Delta E \equiv E_{T_0+1} - E_{T_0} \approx \bar{\nu}(T_0+1)/T_0 \approx 2M(T_0+1). \quad (1)$$

Fallieros, Goulard, and Venter<sup>29</sup> have estimated the splitting to be approximately 7 MeV for <sup>88</sup>Sr ( $T_0=6$ ) and 5 MeV for <sup>90</sup>Zr ( $T_0=5$ ). Titze *et al.*<sup>20</sup> have estimated the splitting in <sup>26</sup>Mg ( $T_0=1$ ) to be  $\Delta E \approx 4.6$  MeV, using

$$\bar{\nu} \approx (T_0/A)60 \text{ MeV}, \quad (2)$$

which agrees reasonably well with the observed grouping of levels. Although the value of  $M$  need not be the same in different nuclei, if one assumes that the difference between the splitting in <sup>26</sup>Mg and in <sup>23</sup>Na and <sup>25</sup>Mg results primarily from the  $T_0$  dependence of Eq. (1), one can get a rough estimate, using Eq. (2), of approximately 3.7 MeV as the separation which might be expected in the latter nuclei.

Another mechanism for splitting the giant resonance in deformed nuclei can be pictured in terms of a hydrodynamic model in which dipole vibrations of different frequency occur along the major and minor axes of the nucleus. This model works well for heavier nuclei,<sup>31</sup> in which distinct resonance peaks are observed with a ratio of peak energies described by the relation

$$E(2)/E(1) = 0.911\eta + 0.089, \quad (3)$$

where  $\eta$  is related to the static quadrupole moment  $Q_0$  by

$$Q_0 = \frac{2}{5} ZR^2(\eta^2 - 1)\eta^{-2/3} = \frac{2}{5} ZR^2\epsilon. \quad (4)$$

In Eq. (4),  $Z$  is the atomic number,  $R$  is the radius of a sphere of equivalent nuclear volume, and  $\epsilon$  is the nuclear eccentricity

$$\epsilon = (b^2 - a^2)/R^2,$$

$$R = (a^2b)^{1/3},$$

where  $a$  is the semiminor axis and  $b$  is the semi-major axis. From the definition of the static quadrupole moment,  $\eta = b/a$ .

Whether or not a classical hydrodynamic model is applicable to nuclei as light as <sup>23</sup>Na and <sup>26</sup>Mg, theoretical calculations based on the shell model have shown<sup>32</sup> that for several  $sd$ -shell nuclei some energy splitting of the dipole state might be expected, with  $\Delta K=0$  states having generally lower energies than  $\Delta K=1$  states, in qualitative agreement with the hydrodynamic model, in which  $\Delta K=0$

corresponds to vibrations along the major axis of the (prolate) nucleus and  $\Delta K = 1$  to vibrations along the minor axes. As a rough estimate of the splitting predicted by Eqs. (3) and (4), we have taken<sup>33</sup>  $Q_0 = 0.1$  and  $0.2$  b for  $^{23}\text{Na}$  and  $^{25}\text{Mg}$ , respectively, and  $R = 1.2 \times A^{1/3}$  F. This implies a splitting of approximately 1.7 MeV for  $^{23}\text{Na}$  and 3.6 MeV for  $^{25}\text{Mg}$ . Although one does not observe, or expect, two well-defined peaks, a broadening of the giant resonance by a few MeV might arise because of nuclear deformation.

### V. CONCLUSIONS

There is an apparent lack of strong structure in the giant-resonance region of  $^{23}\text{Na}$  and  $^{25}\text{Mg}$ . This probably results from too rich a spectrum of di-

pole states to be resolved in the present experiment. The giant resonance in each of these nuclei is fairly broad. The broadening might result from isospin splitting or ground-state deformation or both; both of these effects can be expected to occur, but neither is strong enough to separate the dipole state into distinctly resolved groups of levels.

The integrated total photoneutron cross sections, up to the maximum measured energies fall considerably below the prediction of the dipole sum rule. For  $^{23}\text{Na}$ , however, the photoneutron cross section shows no indication of decreasing at the high-energy limit of the present experiment, while for  $^{25}\text{Mg}$ , the  $(\gamma, p)$  cross section probably accounts for most of the difference. The  $(\gamma, 2n)$  cross sections for both nuclei are smaller than 1 mb up to the maximum measured energy.

†Work performed under the auspices of the U. S. Atomic Energy Commission. A prior report of part of this work appeared in *Bull. Am. Phys. Soc.* **15**, 482 (1970).

<sup>1</sup>S. C. Fultz, J. T. Caldwell, B. L. Berman, R. L. Bramblett, and R. R. Harvey, *Phys. Rev.* **143**, 790 (1966).

<sup>2</sup>J. T. Caldwell, R. R. Harvey, R. L. Bramblett, and S. C. Fultz, *Phys. Letters* **6**, 213 (1963).

<sup>3</sup>S. C. Fultz, R. A. Alvarez, B. L. Berman, M. A. Kelly, D. R. Lasher, T. W. Phillips, and J. McElhinney, *Phys. Rev. C* **4**, 149 (1971).

<sup>4</sup>C. P. Jupiter, N. E. Hansen, R. E. Shafer, and S. C. Fultz, *Phys. Rev.* **121**, 866 (1961); C. R. Hatcher, R. L. Bramblett, N. E. Hansen, and S. C. Fultz, *Nucl. Instr. Methods* **14**, 337 (1961).

<sup>5</sup>R. L. Bramblett, J. T. Caldwell, B. L. Berman, R. R. Harvey, and S. C. Fultz, *Phys. Rev.* **148**, 1198 (1966).

<sup>6</sup>B. L. Berman, R. L. Van Hemert, and C. D. Bowman, *Phys. Rev. Letters* **23**, 386 (1969).

<sup>7</sup>F. W. K. Firk, private communication.

<sup>8</sup>B. L. Berman, J. T. Caldwell, R. R. Harvey, M. A. Kelly, R. L. Bramblett, and S. C. Fultz, *Phys. Rev.* **162**, 1098 (1967); see also previous references described therein.

<sup>9</sup>R. L. Bramblett, J. T. Caldwell, R. R. Harvey, and S. C. Fultz, *Phys. Rev.* **133**, B869 (1964); J. T. Caldwell, R. L. Bramblett, B. L. Berman, R. R. Harvey, and S. C. Fultz, *Phys. Rev. Letters* **15**, 976 (1965).

<sup>10</sup>L. W. Fagg, W. L. Bendel, E. C. Jones, H. F. Kaiser, and T. W. Godlove, *Phys. Rev.* **187**, 1384 (1969).

<sup>11</sup>K. Sato, *J. Phys. Soc. Japan* **18**, 1353 (1963).

<sup>12</sup>D. S. Fielder, L. N. Bolen, and W. D. Whitehead, in *Proceedings of the International Conference on Nuclear Physics, Paris, 1964*, edited by P. Gugenberger (Centre National de la Recherche Scientifique, Paris, France, 1964), p. 1025.

<sup>13</sup>R. Nathans and P. F. Yergin, *Phys. Rev.* **98**, 1296 (1955).

<sup>14</sup>L. Katz, R. N. H. Haslam, J. Goldemberg, and J. G. V. Taylor, *Can. J. Phys.* **32**, 580 (1954).

<sup>15</sup>B. S. Dolbilkin, V. A. Zapevalov, V. K. Korin, L. E. Lazareva, and F. A. Nikolaev, *Izv. Akad. Nauk SSSR Fiz.* **30**, 349 (1966) [transl.: *Bull. Acad. Sci. USSR, Phys. Ser.* **30**, 354 (1966)].

<sup>16</sup>P. P. Singh, R. E. Segel, L. Meyer-Schutzmeister, S. S. Hanna, and R. G. Allas, *Nucl. Phys.* **65**, 577 (1965).

<sup>17</sup>C.-P. Wu, F. W. K. Firk, T. W. Phillips, *Nucl. Phys.* **A147**, 19 (1970); D. V. Webb, E. G. Muirhead, and B. M. Spicer, *ibid.* **A159**, 81 (1970).

<sup>18</sup>R. E. Segel, Z. Vager, L. Meyer-Schutzmeister, P. P. Singh, and R. G. Allas, *Nucl. Phys.* **A93**, 31 (1967).

<sup>19</sup>R. C. Bearse and L. Meyer-Schutzmeister, *Nucl. Phys.* **A116**, 682 (1968).

<sup>20</sup>A. Goldmann, *Z. Physik* **234**, 144 (1970); O. Titze, E. Spamer, and A. Goldman, *Phys. Letters* **24B**, 169 (1967); O. Titze, A. Goldmann, and E. Spamer, *ibid.* **31B**, 565 (1970).

<sup>21</sup>D. V. Webb, B. M. Spicer, and H. Arenhovel, *Phys. Rev.* **165**, 1397 (1967).

<sup>22</sup>F. W. K. Firk, *Nucl. Phys.* **52**, 437 (1964).

<sup>23</sup>J. E. E. Baglin and B. M. Spicer, *Nucl. Phys.* **54**, 549 (1964).

<sup>24</sup>C.-P. Wu, J. E. E. Baglin, F. W. K. Firk, and T. W. Phillips, *Phys. Letters* **29B**, 359 (1969).

<sup>25</sup>G. Dearnaley, D. S. Gemmell, B. W. Hooton, and G. A. Jones, *Nucl. Phys.* **64**, 177 (1965).

<sup>26</sup>W. R. Dodge and W. C. Barber, *Phys. Rev.* **127**, 1746 (1962); E. Finckh, R. Kosiek, K. H. Lindenberger, K. Maier, U. Meyer-Berkhout, M. Schechter, and J. Zimmerer, *Z. Physik* **174**, 337 (1963); W. Hofmann, R. Kosiek, G. Kraft, and R. Mundhenke, *ibid.* **225**, 303 (1969).

<sup>27</sup>P. M. Endt and C. Van der Leun, *Nucl. Phys.* **A105**, 1 (1967).

<sup>28</sup>H. Moringa, *Phys. Rev.* **97**, 444 (1955).

<sup>29</sup>S. Fallieros, B. Goulard, and R. H. Venter, *Phys. Letters* **19**, 398 (1965); B. Goulard, T. A. Hughes, and S. Fallieros, *Phys. Rev.* **176**, 1345 (1968).

<sup>30</sup>C.-P. Wu, F. W. K. Firk, and B. L. Berman, *Phys. Letters* **32B**, 675 (1970).

<sup>31</sup>See, e.g., B. L. Berman, M. A. Kelly, R. L. Bramblett, J. T. Caldwell, H. S. Davis, and S. C. Fultz, *Phys. Rev.* **185**, 1576 (1969).

<sup>32</sup>W. H. Bassichis and F. Scheck, *Phys. Letters* **19**, 509 (1965); *Phys. Rev.* **145**, 771 (1966).

<sup>33</sup>J. N. Dodd and R. W. N. Kinnear, *Proc. Phys. Soc. (London)* **65**, 51 (1960); A. Lurio, *Phys. Rev.* **126**, 1768 (1962).